

Heat Capacity and Thermodynamic Functions of $\text{MnBr}_2 \cdot 4\text{D}_2\text{O}$ and $\text{MnCl}_2 \cdot 4\text{D}_2\text{O}$

J. E. MOORE AND R. A. BUTERA*

*Department of Chemistry, University of Pittsburgh,
Pittsburgh, Pennsylvania 15260*

Received January 30, 1985

The heat capacities of $\text{MnBr}_2 \cdot 4\text{D}_2\text{O}$ and $\text{MnCl}_2 \cdot 4\text{D}_2\text{O}$ have been experimentally determined from 1.4 to 300 K. The smoothed heat capacity and thermodynamic functions ($H_T^\circ - H_0^\circ$) and S_T° are reported for the two compounds over the temperature range 10 to 300 K. The error in the thermodynamic functions at 10 K is estimated to be 3%. Additional error in the tabulated values arising from the heat capacity data above 10 K is thought to be less than 1%. A λ -shaped heat capacity anomaly was observed for $\text{MnCl}_2 \cdot 4\text{D}_2\text{O}$ at 48 K. The entropy associated with the anomaly is 1.2 ± 0.2 J/mole K. © 1985 Academic Press, Inc.

Introduction

Manganese bromide and manganese chloride tetrahydrates have been the subjects of a wide range of investigations. The deuterated analogs have also received some attention in the past (1-3). As part of an ongoing study of the hydrogen bonding in manganese halide hydrates and deuterates, we have experimentally determined the heat capacities of $\text{MnBr}_2 \cdot 4\text{D}_2\text{O}$ and $\text{MnCl}_2 \cdot 4\text{D}_2\text{O}$ from 1.4 to 300 K.

Previously, we reported the existence of a subtle heat capacity anomaly in $\text{MnCl}_2 \cdot 4\text{H}_2\text{O}$ over the temperature range 52 to 90 K (4). The deuterated analog displays a more prominent λ -shaped anomaly with its maximum at 48 K.

As discussed in the previous work (4), we feel these mid-temperature transitions are associated with hydrogen bond ordering. The room temperature structure of

$\text{MnCl}_2 \cdot 4\text{H}_2\text{O}$ is known to contain bifurcated hydrogen bonds (5). Development of a preferred bonding orientation of some of these bifurcated hydrogen bonds as temperature is reduced is not an inconceivable event. What is particularly interesting about the $\text{MnCl}_2 \cdot 4\text{H}_2\text{O}/\text{MnCl}_2 \cdot 4\text{D}_2\text{O}$ system is the gross difference in the heat capacity anomalies; the hydrate displays a broad shallow bump while the deuterate displays a sharp λ -shaped anomaly.

In addition to studying these specific features, we have thermodynamically characterized these materials. It is our present purpose to report the smoothed heat capacity and the thermodynamic functions ($H_T^\circ - H_0^\circ$ and S_T°) over the temperature range 10 to 300 K.

Sample Preparation

Manganese bromide and manganese chloride D_2O solutions were prepared by

* To whom all correspondence should be addressed.

reacting manganese metal¹ with concentrated deuterium bromide and deuterium chloride in D₂O solutions.² The deuterated acids were at least 99 at% D, and were used as the limiting reagents. All manipulations were performed in a glove bag under an inert atmosphere. The tetradeuterates were formed by controlled evaporation of the solutions at room temperature inside a desiccator with freshly baked molecular sieves serving as the desiccant. Crystals approximately 3 to 4 mm in size were obtained and displayed crystal morphology characteristic of the stable α phase (6, 7).

Proton NMR was used to determine the isotopic purity of the deuterated salts. In each case, approximately 5 g of the crystalline material was thermally decomposed, with the waters of deuteration collected in a tared NMR tube. To the known weight of the collected water (≈ 0.5 g), a known amount of anhydrous dimethyl sulfoxide (DMSO) was added (≈ 10 μ l). This provided an accurate internal standard peak equivalent to approximately 1 at% H. Comparison of the integrated water and DMSO peaks yielded the at% H impurity. The NMR measurements were performed on a Varian Anaspect EM360 60 MHz spectrometer. The deuteration levels were found to be 96.2 and 97.9 at% D for the MnBr₂ · 4D₂O and MnCl₂ · 4D₂O, respectively. Based on multiple assays of the crystalline material and on fresh D₂O samples, we expect the accuracy of the measurements to be within ± 0.5 at% D.

Apparatus

Two calorimeters were used in this study. The adiabatic calorimeter which was

¹ Puratronic grade 1 manganese flake, from Johnson Matthey Chemicals Ltd., Orachard Rd., Royston Herts, SG85HE, England; distributed by Alpha Products, Danvers, Mass. 01923.

² Deuterium bromide, 47 wt% solution in D₂O 99+ at% D, deuterium chloride, 37 wt% solution in D₂O 99 at% D, from Aldrich Chemical Co., Milwaukee, Wisc. 53233.

used for temperatures above 10 K has been described elsewhere (4, 8). The sample sizes for this calorimeter were approximately 73 and 39 g of the bromide and chloride, respectively. For temperatures below 10 K, a pulse calorimeter was used. Although a complete description of this apparatus is currently in preparation, a brief description will be given here.

Under computer control, the calorimeter is run in a quasi-isothermal mode. The sample and sample platform are suspended from a comparably massive copper shield (150 g) by superconducting ZrNb wires ($T_c = 14$ K). The sample and shield are alternately heated so that the shield is hot with respect to the sample for the first half of the heat capacity measurement, then cold for the second half. By anticipating the temperature change for the sample (based on the previous heat capacity data point), the shield temperature is chosen such that the initial and final temperatures of the sample are symmetrically disposed about the shield temperature. In this way, the small heat leak between the sample and shield is nearly balanced over the heat capacity measurement cycle.

The sample thermometry is based on a germanium resistance thermometer with a nominal resistance of 1 k Ω at 4 K. This thermometer was calibrated with secondary standards maintained by the manufacturer.³ A typical temperature step size is $T/20$, though a constant heat mode is often used, particularly in the case of measuring a λ transition.

Since the calorimeter was originally designed to measure the heat capacities of 5- to 10-g metal samples, the heat capacity equivalent sample size for the manganese salts is very small. For this study, single crystal samples were used with masses in the range 50–100 mg. These small masses and the nominal 2–3 mg of silicone stop-

³ Germanium resistance thermometer, from Cryo-Cal, Inc., Riviera Beach, Fla. 33404.

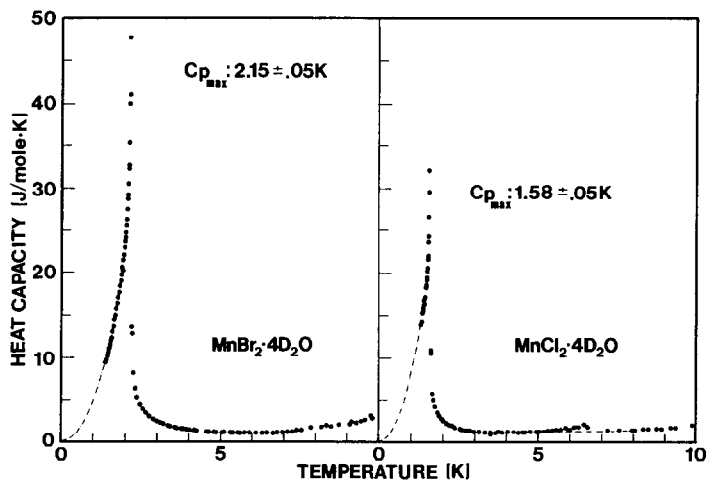


FIG. 1. Experimental heat capacity data for $\text{MnBr}_2 \cdot 4\text{D}_2\text{O}$ and $\text{MnCl}_2 \cdot 4\text{D}_2\text{O}$ below 10 K.

cock grease used to attach the crystals to the copper sample platform are the principal sources of inaccuracy in the data. Further, from measuring the temperature of the heat capacity maxima near the Néel points for several previously studied salts ($\text{MnCl}_2 \cdot 4\text{H}_2\text{O}$, $\text{MnBr}_2 \cdot 4\text{H}_2\text{O}$, and $\text{CoCl}_2 \cdot 6\text{H}_2\text{O}$), (9–11), we suspect there is approximately a +0.03 K shift in the thermometer calibration. We are currently in the process of replacing the germanium thermometer and redesigning the sample platform to accommodate larger salt samples. Ultimately we expect this calorimeter to produce data accurate to better than 1%, though currently, the data is believed to be only accurate to about 2 or 3%.

Results and Discussion

Figure 1 shows the experimental heat capacity data⁴ for temperatures below 10 K. The dot-dashed lines from the low tempera-

ture limits of the data to 0 K are the extrapolations used to reference the thermodynamic functions to absolute zero. In splineing these lines, the low-temperature behavior of the corresponding hydrates was used as a guide. For the hydrates, experimental heat capacity has been reported down to 0.3 K (12).

The small peak in the $\text{MnCl}_2 \cdot 4\text{D}_2\text{O}$ experimental data near 6.5 K is the antiferromagnetic transition of $\text{MnCl}_2 \cdot 2\text{D}_2\text{O}$ (13). This contamination is due to the loss of D_2O from the surface of the crystal during the calorimeter cool down. The dot-dashed line which undercuts this data was used in the smoothed heat capacity curve from which the thermodynamic functions were obtained. Based on the entropy content of this peak, the $\text{MnCl}_2 \cdot 2\text{D}_2\text{O}$ impurity was less than 1% by mass.

As previously mentioned, we have also determined the temperatures of the heat capacity maxima near the Néel points for $\text{MnBr}_2 \cdot 4\text{H}_2\text{O}$ and $\text{MnCl}_2 \cdot 4\text{H}_2\text{O}$. In a comparison of the shift in heat capacity maxima

⁴ See NAPS document 04323 for 28 pages of supplementary material. Order from ASIS/NAPS, Microfiche Publications, P.O. Box 3513, Grant Central Station, New York, N.Y. 10163. Remit in advance \$4.00 for microfiche copy or for photocopy, \$7.75 up to 20 pages plus \$0.30 for each additional page. All orders must be prepaid. Institutions and organizations may order by purchase order. However, there is a billing

and handling charge for this service of \$15. Foreign orders add \$4.50 for postage and handling, for the first 20 pages, and \$1.00 for each additional 10 pages of material. There is a \$1.50 charge for postage of any microfiche orders.

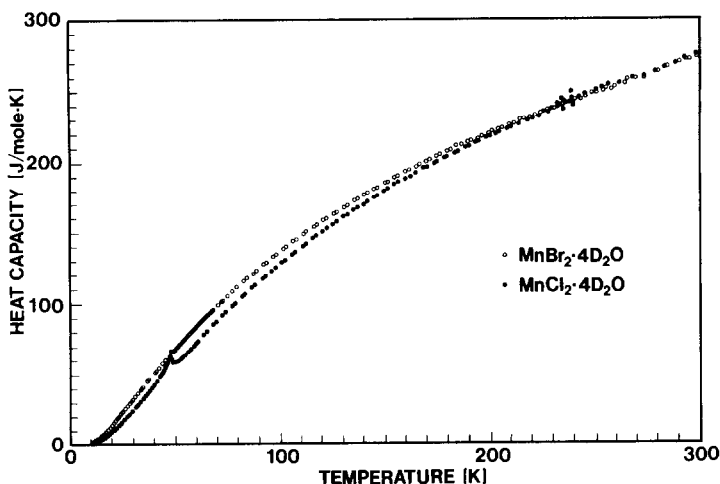


FIG. 2. Experimental heat capacity data for MnBr₂ · 4D₂O and MnCl₂ · 4D₂O above 10 K.

with deuteration, we find -1% and -4% shifts resulting from deuteration for the bromide and chloride, respectively. This is in fair agreement with the work of Yue and Turrell (3) where they found -1.1% and -2.3% shifts, respectively.

Figure 2 shows the experimental heat capacity data⁴ for temperatures above 10 K. The λ -shaped anomaly at 48 K is seen to be a relatively minor feature on the MnCl₂ · 4D₂O heat capacity curve.

Our method of smoothing the experimental data involves the use of a draftman's spline, and has been detailed elsewhere (4). Figures 3 and 4 show the percent deviation between the experimental data and the smoothed heat capacity curves for the two compounds. For these plots,

$$\Delta\%C_p = \frac{\text{Smooth } C_p - \text{experimental } C_p}{\text{smooth } C_p} \cdot 100\%$$

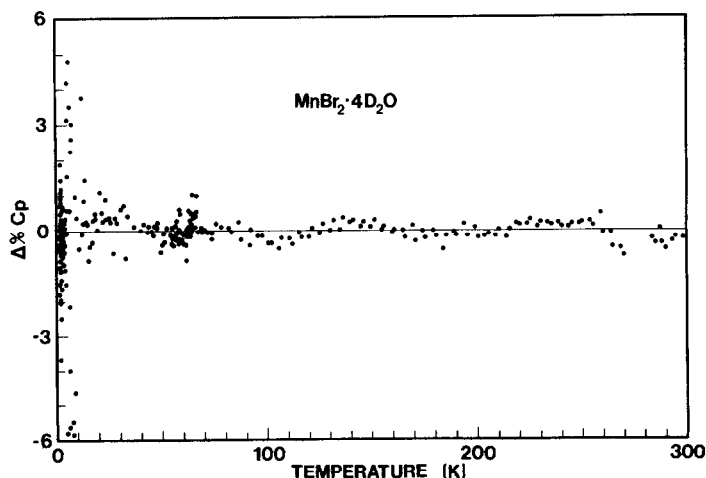


FIG. 3. Percentage deviation between smoothed and experimental heat capacity data for MnBr₂ · 4D₂O.

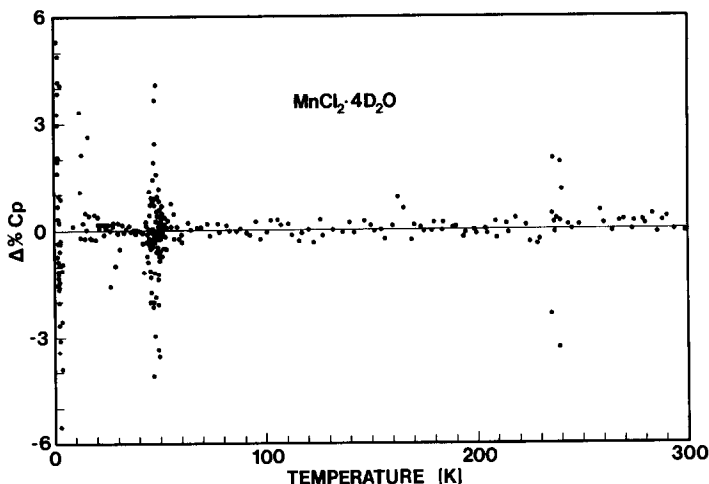


FIG. 4. Percentage deviation between smoothed and experimental heat capacity data for $\text{MnCl}_2 \cdot 4\text{D}_2\text{O}$.

Tables I and II give the smoothed heat capacity and thermodynamic functions ($H_T^\circ - H_0^\circ$) and S_T° for $\text{MnBr}_2 \cdot 4\text{D}_2\text{O}$ and $\text{MnCl}_2 \cdot 4\text{D}_2\text{O}$, respectively. The reported

thermodynamic functions were obtained numerically from the smoothed heat capacity curves. The heat capacity data density used in these evaluations was sufficiently high so that insignificant error was introduced due to the numerical techniques.

Based on the required extrapolation to absolute zero and the accuracy of the experimental heat capacity data below 10 K, we estimate the error in the thermodynamic functions at 10 K to be approximately 3%. Additional error in the tabulated values arising from the heat capacity data above 10 K is thought to be less than 1%.

Figure 5 shows the λ -shaped heat capacity anomaly in detail. Here, the data points are shown as bars indicating the initial and final temperatures of the individual measurements. The smaller bars which are required to resolve the shape of the feature are also necessarily less accurate and display a large degree of scatter. The dot-dashed line is our estimated blank heat capacity curve which is based on a sixth-order polynomial least-squares fit to the smoothed heat capacity curve adjacent to the anomaly region. The entropy associated with this feature is $1.2 \pm 0.2 \text{ J/mole K}$.

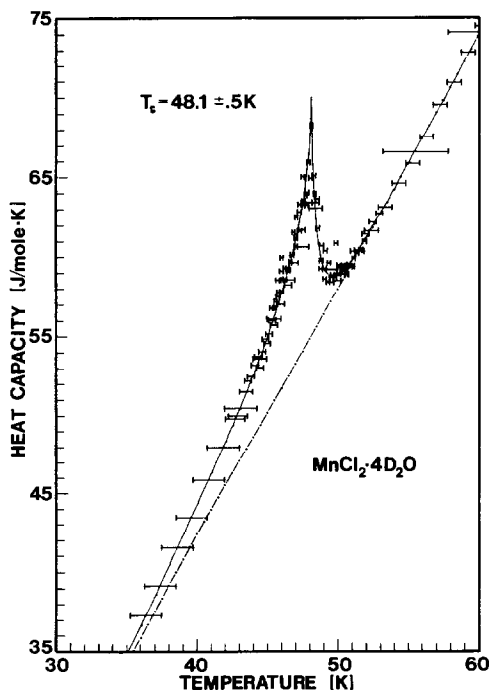


FIG. 5. Heat capacity anomaly in $\text{MnCl}_2 \cdot 4\text{D}_2\text{O}$.

TABLE I
SMOOTH THERMODYNAMIC FUNCTIONS FOR
MnBr₂ · 4D₂O

<i>T</i> (K)	<i>C_p</i> (J/mole K)	<i>H_T^o-H₀^o</i> (J/mole)	<i>S_T^o</i> (J/mole K)
10.00	2.62	32.81	14.78
15.00	7.79	57.22	16.69
20.00	15.80	115.41	19.98
25.00	25.04	217.43	24.49
30.00	34.58	366.26	29.89
35.00	43.93	563.03	35.94
40.00	52.70	804.52	42.38
45.00	61.50	1089.91	49.09
50.00	70.02	1419.22	56.02
55.00	78.01	1789.35	63.07
60.00	85.79	2198.95	70.19
65.00	93.50	2646.96	77.36
70.00	100.45	3131.88	84.55
75.00	107.13	3650.93	91.71
80.00	113.70	4203.56	98.83
85.00	120.12	4787.72	105.92
90.00	126.12	5403.32	112.95
95.00	131.80	6048.28	119.93
100.00	137.32	6721.06	126.83
110.00	148.15	8148.62	140.42
120.00	158.54	9682.51	153.76
130.00	168.44	11317.81	166.85
140.00	177.52	13048.33	179.67
150.00	185.88	14865.96	192.21
160.00	193.75	16764.41	204.46
170.00	201.38	18740.60	216.43
180.00	208.48	20790.23	228.15
190.00	215.15	22908.76	239.60
200.00	221.38	25091.69	250.80
210.00	227.42	27335.90	261.74
220.00	233.26	29639.54	272.46
230.00	238.85	32000.39	282.95
240.00	244.23	34415.82	293.23
250.00	249.48	36884.31	303.31
260.00	254.66	39405.07	313.19
270.00	259.77	41977.28	322.90
273.15	261.40	42798.09	325.92
280.00	264.82	44600.39	332.44
290.00	269.60	47272.68	341.82
298.15	273.45	49485.71	349.34
300.00	274.32	49992.39	351.04

The uncertainty in this number is based on variations in the entropy with changes in the least-squares fitting of the blank curve.

If we assume a deuterium bond order-

disorder transition, then the entropy involved would be $R \ln 2$ /mole of participating bonds. The entropy found is close to $\frac{1}{4}R \ln 2$ (1.4 J/mole K), which corresponds to

TABLE II
SMOOTH THERMODYNAMIC FUNCTIONS FOR
MnCl₂ · 4D₂O

<i>T</i> (K)	<i>C_p</i> (J/mole K)	<i>H_T^o-H₀^o</i> (J/mole)	<i>S_T^o</i> (J/mole K)
10.00	1.66	25.82	16.14
15.00	4.60	40.27	17.27
20.00	10.15	76.10	19.29
25.00	17.45	144.47	22.31
30.00	25.71	252.11	26.21
35.00	34.79	403.14	30.85
40.00	44.30	600.66	36.11
45.00	55.01	847.87	41.92
50.00	58.83	1149.10	48.27
55.00	65.90	1459.43	54.18
60.00	73.97	1808.74	60.25
65.00	81.74	2198.32	66.48
70.00	89.10	2625.53	72.81
75.00	96.23	3088.93	79.20
80.00	102.90	3586.74	85.63
85.00	109.48	4117.72	92.06
90.00	115.96	4681.41	98.51
95.00	122.27	5277.07	104.95
100.00	128.35	5903.72	111.37
110.00	139.78	7244.87	124.15
120.00	150.65	8697.49	136.78
130.00	161.08	10256.65	149.25
140.00	170.94	11917.38	161.56
150.00	180.18	13673.36	173.67
160.00	188.85	15519.06	185.58
170.00	196.98	17451.09	197.29
180.00	204.52	19459.08	208.76
190.00	211.64	21539.99	220.01
200.00	218.45	23690.54	231.04
210.00	224.98	25907.87	241.86
220.00	231.20	28189.04	252.47
230.00	237.12	30530.70	262.88
240.00	242.78	32930.31	273.09
250.00	248.48	35386.89	283.12
260.00	254.07	37899.55	292.97
270.00	259.65	40468.05	302.66
273.15	261.41	41288.71	305.69
280.00	265.24	43092.50	312.21
290.00	270.90	45773.04	321.61
298.15	275.49	47999.62	329.18
300.00	276.53	48510.24	330.89

two bonds per unit cell. This would appear to be the smallest entropy change consistent with the ordering of one water molecule and the periodic nature of the crystal.

Although we reported that the entropy of the assumed analogous transition in $\text{MnCl}_2 \cdot 4\text{H}_2\text{O}$ is of the order 0.4 J/mole K, it could be much closer to the value reported here for $\text{MnCl}_2 \cdot 4\text{D}_2\text{O}$. The principal difficulty is accurately determining a suitable blank heat capacity curve for the hydrate. Apparently there is a difference in the specific details of the transitions, but we are unable to claim that there is a difference in the entropy content between the two. Examination of this system with a microscopically sensitive technique would be extremely useful in helping to understand these transitions.

Acknowledgment

One of the authors (JEM) would like to thank the Andrew Mellon Foundation for its support in the form of a predoctoral fellowship.

References

1. R. A. BUTERA, L. M. CORLISS, J. M. HASTINGS, R. THOMAS, AND D. MUKAMEL, *Phys. Rev. B* **24**, 1244 (1981).
2. B. G. TURRELL AND C. L. YUE, *Canad. J. Phys.* **49**, 2520 (1971).
3. C. L. YUE AND B. G. TURRELL, *Solid State Commun.* **8**, 1261 (1970).
4. J. E. MOORE AND R. A. BUTERA, *J. Solid State Chem.* **59**, 81 (1985).
5. Z. M. EL SAFFAR AND G. M. BROWN, *Acta Crystallogr. B* **27**, 66 (1971).
6. K. SUDARSANAN, *Acta Crystallogr. B* **31**, 2720 (1975).
7. A. SALKIN, D. J. FORRESTER, AND D. H. TEMPLETON, *Inorg. Chem.* **3**, 529 (1964).
8. D. J. GERMANO, R. A. BUTERA, S. G. SANKAR, AND K. A. GSCHNEIDER, JR., *J. Appl. Phys.* **50**, 7495 (1979).
9. T. A. REICHERT, R. A. BUTERA, AND E. J. SCHILLER, *Phys. Rev. B* **1**, 4446 (1970).
10. L. W. KREPS AND S. A. FRIEDBERG, *J. Low Temp. Phys.* **26**, 317 (1977).
11. W. K. ROBINSON AND S. A. FRIEDBERG, *Phys. Rev.* **117**, 402 (1960).
12. A. R. MIEDEMA, R. F. WIELINGA, AND W. J. HUSIKAMP, *Physica* **31**, 835 (1965).
13. J. N. MCEARNEY, S. MERCHANT, AND R. L. CARLIN, *Inorg. Chem.* **12**, 906 (1973).